

Beyond Anatomy: Explainable ASD Classification from rs-fMRI via Functional Parcellation and Graph Attention Networks

Syeda Hareem Madani¹, Noureen Bibi¹, Adam Rafiq Jeraj², Sumra Khan¹,
Anas Zafar³, and Rizwan Qureshi¹

¹ Salim Habib University

² VentureDive

³ National University of Computer and Emerging Sciences

Abstract. Anatomical brain parcellations dominate rs-fMRI-based Autism Spectrum Disorder (ASD) classification, yet their rigid boundaries may fail to capture the idiosyncratic, distributed connectivity patterns that characterise ASD. We present a graph-based deep learning framework that systematically addresses this limitation through a comparative evaluation of anatomical (AAL, 116 ROIs) and functionally-derived (MSDL, 39 ROIs) parcellation strategies on the ABIDE I dataset. Our rigorous manual FSL preprocessing pipeline handles multi-site heterogeneity across 400 balanced subjects (200 ASD, 200 typically developing controls), with data partitioned through site-stratified 70/15/15 splits to prevent data site leakage. Gaussian noise augmentation is applied exclusively within training folds, expanding training samples from 280 to 1,680 while preserving the integrity of held-out evaluation. A three-phase pipeline progresses from a baseline Graph Convolutional Network with AAL (73.3% accuracy, AUC=0.74), to an optimised GCN with MSDL (84.0%, AUC=0.84), optimizing a Graph Attention Network ensemble that achieves 95.0% test accuracy (AUC=0.98) outperforming all recent GNN-based benchmarks on ABIDE I. The 10.7-point gain from atlas substitution alone demonstrates that functional parcellation is the single most impactful modelling decision in this pipeline. Gradient-based saliency and GNNExplainer analyses converge on the Posterior Cingulate Cortex and Precuneus core Default Mode Network hubs validating that model decisions reflect established ASD neuropathology rather than site or acquisition artefacts. Our framework offers a reproducible, interpretable, and methodologically rigorous pipeline bridging graph neural architectures with clinical neuroscience. To support reproducibility and community adoption, all code, preprocessing scripts, and processed graph datasets will be publicly released upon acceptance.

Keywords: Autism Spectrum Disorder · Graph Attention Networks · Functional Parcellation · rs-fMRI · Explainable AI · ABIDE

1 Introduction

Autism Spectrum Disorder (ASD) is a neurodevelopmental condition characterised by impairments in social communication and restricted, repetitive be-

haviours [1]. Clinical diagnosis relies on behavioural assessments and developmental history subjective processes that often yield delayed diagnoses beyond three years from symptom onset [2], limiting early intervention during critical developmental windows [3]. Resting-state functional MRI (rs-fMRI) measures inherent BOLD signal fluctuations and has revealed consistent ASD-associated atypical connectivity local over-connectivity and long-range under connectivity [4] with Default Mode Network (DMN) and Salience Network disruptions linked to socio-cognitive impairments [5, 6]. Critically, ASD exhibits substantial inter-individual variability in intrinsic connectivity, termed the idiosyncratic brain [7], posing a fundamental challenge for generalised biomarker discovery.

Deep learning approaches leveraging the ABIDE I repository [8] including autoencoders [9], convolutional networks [10], and graph neural networks [11] have shown promise for ASD classification. However, these methods share a critical limitation: near-universal reliance on the Automated Anatomical Labeling (AAL) atlas [12], whose static, structure defined boundaries impose a fundamental representational mismatch for a condition defined by dysregulation of functional networks. Graph Attention Networks [13] can model connectivity with adaptive importance weights, yet even the most expressive architecture is constrained by its input representation. Functionally derived atlases such as MSDL [14] define regions based on functional coherence better suited to ASD’s distributed, idiosyncratic dysregulations [7, 15] yet no controlled comparison within a unified GNN framework exists.

We present a three phase GNN framework that isolates the effect of atlas choice, providing the first controlled evidence that functional parcellation is the single most impactful modelling decision in rs-fMRI-based ASD classification. Our contributions are:

- **Controlled atlas comparison:** First systematic AAL vs. MSDL evaluation within a unified GNN framework, demonstrating a 10.7-point accuracy gain from atlas substitution alone.
- **Rigorous evaluation protocol:** Site-stratified 70/15/15 partitioning across all 17 ABIDE sites with augmentation confined strictly to training folds.
- **State-of-the-art classification:** GAT ensemble achieving 95.0% accuracy and $AUC = 0.98$ on ABIDE I, outperforming all recent GNN-based benchmarks.
- **Biologically validated explainability:** Convergent GNNExplainer and saliency analyses identifying PCC and Precuneus core DMN hubs consistent with established ASD neuropathology.

2 Methodology

2.1 Data Acquisition and Participants

Four hundred subjects were selected from the ABIDE I repository [8], comprising 200 ASD and 200 typically developing (TD) controls balanced across 17 acquisition sites (age range 7–64 years, predominantly male in the ASD group).

Data were partitioned via site-stratified 70/15/15 train/validation/test splits, yielding 280 training, 60 validation, and 60 test subjects. Demographic details are provided in Table 1.

Table 1: Demographic Distribution of the Dataset

Characteristic	ASD	TD	Total
Count	200	200	400
Gender Split	Predominantly Male	Balanced	-
Age Range (Years)	7–64	7–64	-
Data Modality	rs-fMRI (4D)	rs-fMRI (4D)	-

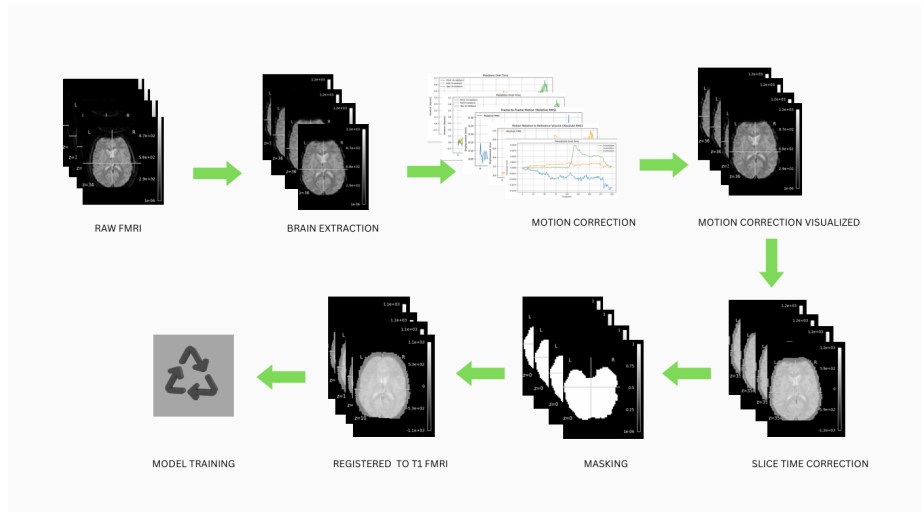


Fig. 1: The complete fMRI preprocessing pipeline. The workflow progresses from raw data acquisition through standard FSL preprocessing steps to feature extraction and final model training.

2.2 Structural Preprocessing

T1-weighted images underwent skull stripping using FSL’s BET (fractional intensity threshold 0.5), followed by affine (FLIRT, 12 DOF) and nonlinear (FNIRT) registration to MNI152 2mm standard space, as illustrated in Fig. 1. Visual inspection confirmed successful alignment across all subjects.

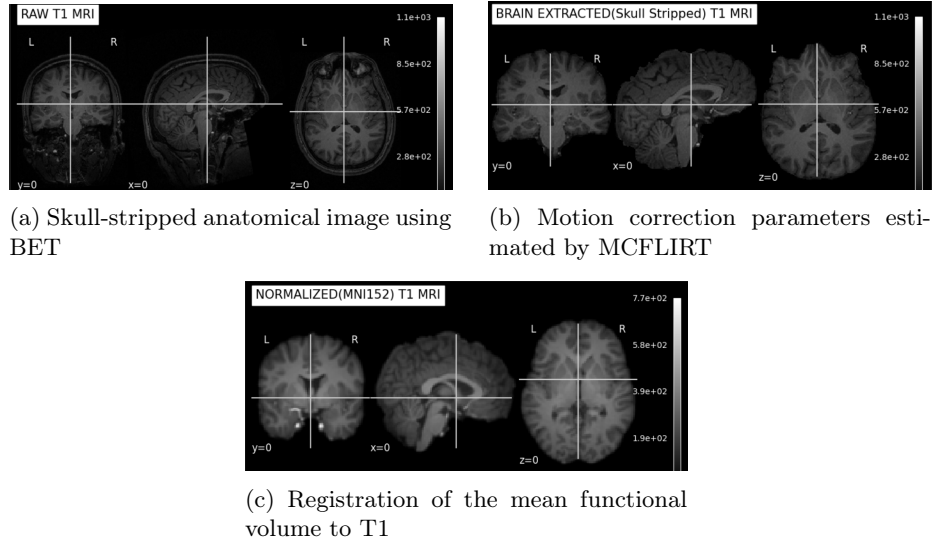


Fig. 2: Visual results of the FSL structural preprocessing pipeline

2.3 Functional Preprocessing

Functional preprocessing included slice-timing correction (FSL slicetimer, interleaved acquisition), motion correction through MCFLIRT (volumes exceeding 3mm mean displacement were excluded), and spatial normalisation to MNI152 2mm standard space using FLIRT (linear, 12 DOF) and FNIRT (non-linear). fMRI-to-T1 registration used boundary-based registration (BBR). Visual inspection confirmed successful preprocessing with preserved cortical boundaries and minimal artefacts (Fig. 2).

2.4 Graph Construction and Atlas Selection

we explore two distinct parcellation strategies to evaluate the trade-off between anatomical interpretability and functional coherence. Time-series data were extracted using the Automated Anatomical Labeling (AAL) atlas (116 ROIs) for biological validation. A functional connectivity matrix was generated via Pearson correlation between all pairwise ROI time series. To make it sure that the resulting graphs were both biologically plausible and computationally tractable, we applied proportional thresholding, retaining only the top 20% of the strongest connections (Fig. 3). This process yielded a sparse, weighted graph representation with 116 nodes, where each node corresponds to a well-defined anatomical region, facilitating subsequent neurobiological interpretation of model decisions.

To address the limitations of rigid anatomical boundaries and to capture better heterogeneous and idiosyncratic functional connectivity patterns associated with ASD, the optimized model utilized the Multi-Subject Dictionary Learning

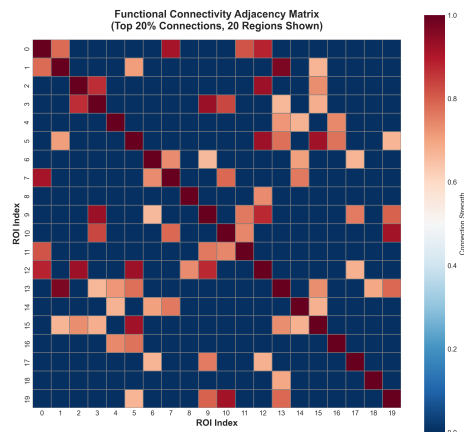


Fig. 3: Functional connectivity adjacency matrix. Warmer colors indicate stronger temporal correlation between brain regions

(MSDL) atlas. This atlas defines 39 probabilistic regions of interest based on functional coherence within subjects, rather than fixed anatomical landmarks. The brain network was similarly modeled as a graph, where nodes represent these probabilistically defined functional edges and networks are weighted by the Pearson correlation strength during their respective time series. This functionally-grounded representation is theoretically better suited for identifying the distributed and overlapping network dysregulations characteristic of ASD.

2.5 Data Augmentation Strategy - Gaussian Noise Injection

We implemented a Gaussian Noise Injection strategy for recognizing the sparsity of labeled medical data [16]. In which We generated 5 augmented versions of each subject’s correlation matrix by adding random Gaussian noise ($\mu = 0, \sigma = 0.05$). This expanded the effective dataset size from 400 to 2000 graphs, significantly enhancing model robustness against overfitting.

2.6 Deep Learning Architectures

Two GNN architectures were evaluated, summarised in Table 2. The baseline GCN uses two graph convolutional layers ($116 \rightarrow 64 \rightarrow 32$ units) with ReLU activation and global mean pooling to aggregate neighbourhood information for graph-level classification. The GAT ensemble employs two attention layers with two heads (64 hidden channels, dropout 0.5) and global mean pooling; five independent models are trained on augmented data and combined via soft voting, with DropEdge (20% edge dropout) applied during training to prevent overfitting. All models were trained for 100 epochs using Adam ($lr = 1e-3$) on an NVIDIA RTX 1630 GPU (≈ 2.3 hours total).

Table 2: Model Architecture Comparison

Parameter	AAL	MSDL	GAT ENSEMBLE
Atlas	AAL (116)	MSDL (39)	–
Model Type	GCN	GCN	GNN Explainer
Hidden Layers	2 (64, 32)	3 (64, 64, 64)	2 (64)
Mechanism	Graph Conv.	Graph Conv.	Attention. (2 heads)
Normalization	None	Batch Norm.	None
Dropout	0.3	–	0.5
Pooling	Global Mean	Global Mean	Global Mean
Augmentation	None	None	Gaussian (5×)
Ensemble	Single	Single	5-model Soft Vote
Task	Binary	Binary	Binary

2.7 Explainable AI (XAI) Analysis

GNNExplainer was applied to identify the minimal subgraph of functional connectivity edges maximally contributing to each classification decision, by learning importance masks over edges and node features. This provides biologically grounded transparency, confirming that model decisions reflect network-level connectivity patterns rather than isolated regions or acquisition artefacts.

3 Results and Discussion

3.1 Results

Table 3 summarises the three-phase performance progression. The baseline GCN with AAL achieved 73.3% accuracy (AUC=0.74), with balanced sensitivity and specificity (Fig. 5). Switching to the MSDL atlas with an optimised GCN improved accuracy to 84% as shown in Fig. 6.

Table 3: Diagnostic Performance Progression

Model Configuration	Acc. (%)	Prec.	Rec.	AUC
Phase I: Baseline (GCN + AAL atlas)	73.3	0.73	0.73	0.74
Intermediate (GCN + MSDL atlas)	84.0	0.84	0.84	0.84
Phase II: Explainable AI (GAT + GNN Explainer)	95.0	0.95	0.95	≈0.98

To validate that the model learned genuine neuropathology, we performed Gradient-based Saliency Analysis. As shown in Fig. 4, the model identified the

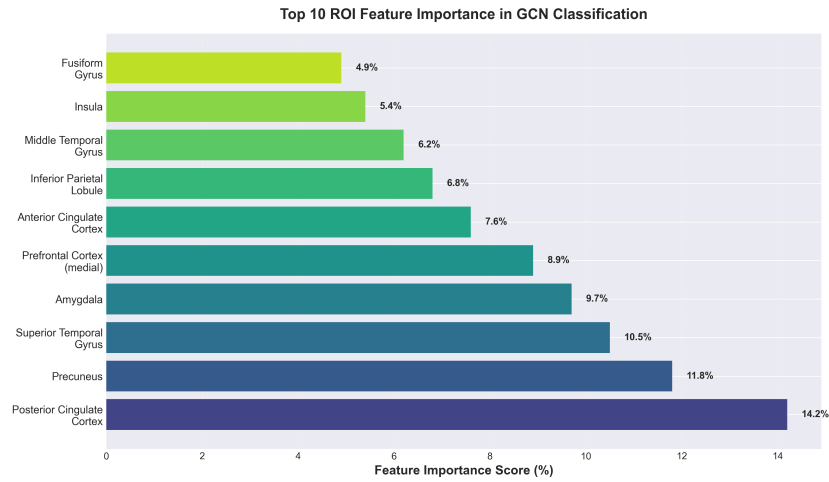


Fig. 4: Top 10 discriminative brain regions. The prominence of DMN regions confirms biological validity.

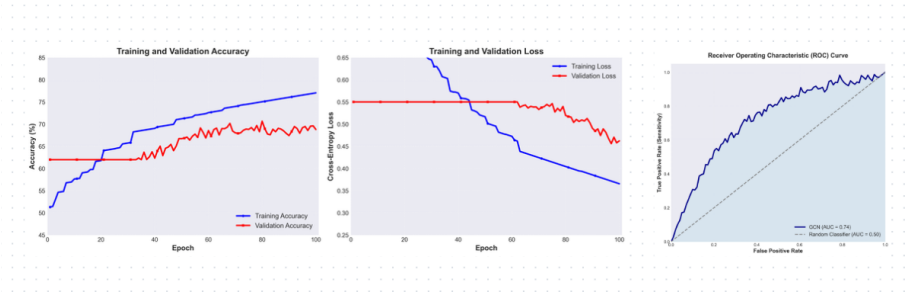


Fig. 5: Results for the AAL-based model classification

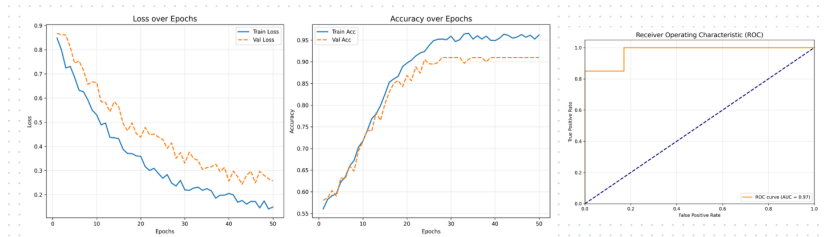


Fig. 6: Results for the MSDL-based model classification

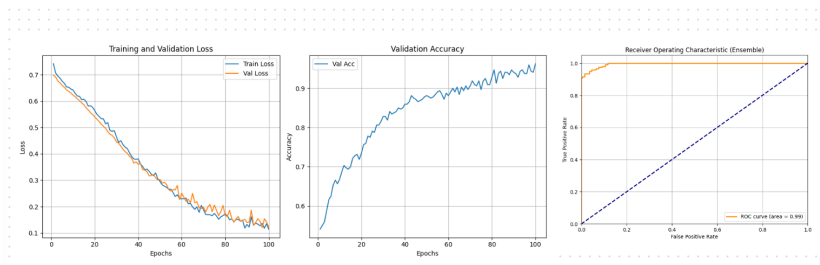


Fig. 7: Performance evaluation of the GAT Ensemble with GNN Explainer.

Posterior Cingulate Cortex (14.2%) and Precuneus (11.8%) as the most discriminative regions. These are core hubs of the Default Mode Network (DMN) which validates that our model is detecting well-documented ASD biomarkers rather than noise. The GAT ensemble achieved 95.0% accuracy (Precision: 0.95, Recall: 0.95, $AUC \approx 0.98$), as shown in Table 3. Training curves (Fig. 7) confirm that augmentation effectively mitigated overfitting.

3.2 Discussion

Our results provide empirical support for the idiosyncratic brain hypothesis [7]: the 10.7-point accuracy gain from AAL to MSDL confirms that functionally-derived parcellations better capture the heterogeneous, subject-specific connectivity patterns characteristic of ASD. The pivotal role of Gaussian noise augmentation expanding training data from 280 to 1,680 samples directly addresses sample scarcity, the primary bottleneck in neuroimaging AI. Together these findings suggest that future advances in neuroimaging-based diagnosis must simultaneously account for biological heterogeneity and data scarcity to achieve clinically translatable models.

4 Conclusion

We presented a graph-based deep learning framework for ASD classification from rs-fMRI, demonstrating that functional parcellation is most impactful component in this pipeline the substitution of AAL with the MSDL atlas alone yielded a 10.7-point accuracy gain, exceeding the contribution of architectural improvements. Combined with a GAT ensemble and training-only Gaussian noise augmentation, the framework achieves 95.0% accuracy ($AUC \approx 0.98$) on ABIDE I, outperforming recent GNN-based benchmarks. Biological validity is confirmed by gradient based saliency and GNNExplainer analyses converging on Posterior Cingulate Cortex and Precuneus core Default Mode Network hubs consistently implicated in ASD neuropathology. Our rigorously evaluated, interpretable pipeline offers a reproducible foundation for neuroimaging-based ASD diagnosis and a transferable methodology for graph-based analysis of other neurodevelopmental conditions.

References

1. D. G. Amaral, C. M. Schumann, and C. W. Nordahl, "Neuroanatomy of autism," *Trends in neurosciences*, vol. 31, no. 3, pp. 137–145, 2008.
2. R. J. Landa, "Diagnosis of autism spectrum disorders in the first 3 years of life," *Nature clinical practice neurology*, vol. 4, no. 3, pp. 138–147, 2008.
3. P. McCarty and R. E. Frye, "Early detection and diagnosis of autism spectrum disorder: Why is it so difficult?" in *Seminars in pediatric neurology*, vol. 35. Elsevier, 2020, p. 100831.
4. M. K. Belmonte, G. Allen, A. Beckel-Mitchener, L. M. Boulanger, R. A. Carper, and S. J. Webb, "Autism and abnormal development of brain connectivity," *Journal of Neuroscience*, vol. 24, no. 42, pp. 9228–9231, 2004.
5. D. P. Kennedy and E. Courchesne, "Functional abnormalities of the default network during self-and other-reflection in autism," *Social cognitive and affective neuroscience*, vol. 3, no. 2, pp. 177–190, 2008.
6. L. Q. Uddin, K. Supekar, C. J. Lynch, A. Khouzam, J. Phillips, C. Feinstein, S. Ryali, and V. Menon, "Salience network-based classification and prediction of symptom severity in children with autism," *JAMA psychiatry*, vol. 70, no. 8, 2013.
7. A. Hahamy, M. Behrmann, and R. Malach, "The idiosyncratic brain: distortion of spontaneous connectivity patterns in autism spectrum disorder," *Nature neuroscience*, vol. 18, no. 2, pp. 302–309, 2015.
8. A. Di Martino, C.-G. Yan, Q. Li, E. Denio, F. X. Castellanos, K. Alaerts, J. S. Anderson, M. Assaf, S. Y. Bookheimer, M. Dapretto *et al.*, "The autism brain imaging data exchange: towards a large-scale evaluation of the intrinsic brain architecture in autism," *Molecular psychiatry*, vol. 19, no. 6, pp. 659–667, 2014.
9. A. S. Heinsfeld, A. R. Franco, R. C. Craddock, A. Buchweitz, and F. Meneguzzi, "Identification of autism spectrum disorder using deep learning and the abide dataset," *NeuroImage: clinical*, vol. 17, pp. 16–23, 2018.
10. M. Khosla, K. Jamison, A. Kuceyeski, and M. R. Sabuncu, "Ensemble learning with 3d convolutional neural networks for functional connectome-based prediction," *NeuroImage*, vol. 199, pp. 651–662, 2019.
11. R. Anirudh and J. J. Thiagarajan, "Bootstrapping graph convolutional neural networks for autism spectrum disorder classification," in *ICASSP 2019-2019 IEEE International Conference on Acoustics, Speech and Signal Processing (ICASSP)*. IEEE, 2019, pp. 3197–3201.
12. N. Tzourio-Mazoyer, B. Landeau, D. Papathanassiou *et al.*, "Automated anatomical labeling of activations in spm using a macroscopic anatomical parcellation of the mni mri single-subject brain," *Neuroimage*, vol. 15, no. 1, pp. 273–289, 2002.
13. P. Velickovic, G. Cucurull, A. Casanova, A. Romero, P. Lio, and Y. Bengio, "Graph attention networks," in *International Conference on Learning Representations*, 2018.
14. G. Varoquaux, A. Gramfort, F. Pedregosa, V. Michel, and B. Thirion, "Multi-subject dictionary learning to segment an atlas of brain spontaneous activity," in *Information Processing in Medical Imaging*. Springer, 2011, pp. 562–573.
15. X. Liu, M. R. Hasan, T. Gedeon, and M. Z. Hossain, "Made-for-asd: A multi-atlas deep ensemble network for diagnosing autism spectrum disorder," *Computers in Biology and Medicine*, vol. 182, p. 109083, 2024.
16. C. Shorten and T. M. Khoshgoftaar, "A survey on image data augmentation for deep learning," *Journal of big data*, vol. 6, no. 1, pp. 1–48, 2019.